$$\vec{a}=(-z_+^2+z_-^2,\ -i(z_+^2+z_-^2),\ 2z_+z_-), \tag{59}$$

and $\phi_{kq}(z)$ is defined as

$$\phi_{kq}(z)=\frac{z_+^{k+q}z_-^{k-q}}{\sqrt{(k+q)!(k-q)!}}. \tag{60}$$

If we differentiate both sides of Eq. (58), we obtain

$$\frac{\vec{a}}{2}\frac{(\vec{a}\cdot\vec{r})^{(k-1)}}{2^{k-1}(k-1)!}=\sum_q\phi_{kq}(z)\nabla C^{[k]}. \tag{61}$$

If we make the coefficients of $\phi_{kq}(z)$ of Eq. (61) zero, the following relations are obtained:

$$\begin{aligned}
&\nabla_1^{[1]}C_q^{[k]}=\sqrt{\frac{(k-q)(k-q-1)}{2}}\,C_{q+1}^{[k-1]},\\
&\nabla_0^{[1]}\nabla_q^{[k]}=-\sqrt{(k^2-q^2)}C_{q+1}^{[k-1]},\\
&\nabla_{-1}^{[1]}C_q^{[k]}=\sqrt{\frac{(k+q)(k+q-1)}{2}}\,C_{q-1}^{[k-1]}.
\end{aligned} \tag{62}$$

On the other hand, by the well known vector coupling theory, $\nabla_{q'}^{[1]}C_q^{[k]}$ can be decomposed into irreducible products $[\nabla^{[1]}C^{[k]}]_{q+q'}^{[K]}$ with the expansion coefficients given by the Wigner coefficients as follows:

$$\begin{aligned}
\nabla_{q'}^{[1]}C_q^{[k]}&=\sum_K(1q'kq|Kq+q')[\nabla^{[1]}C^{[k]}]_{q+q'}^{(K)}\\
&=(1q'kq|k-1q+q')[\nabla^{[1]}C^{[k]}]_{q+q'}^{[k-1]}.
\end{aligned} \tag{63}$$

From Eqs. (62) and (63), we obtain Eq. (21).

References

1. Howard, M. J.; Smith, I. W. M. *Prog. React. Kinet.* **1983**, *12*, 55.
2. (a) Quack, M.; Tröe, J. *Ber. Bunsenges. Phys. Chem.* **1974**, *78*, 240. (b) Quack, M.; Tröe, J. *ibid*, **1983**, *81*, 329. (c) Tröe, J. *J. Chem. Phys.* **1983**, *79*, 6017.
3. (a) Wardlaw, D. M.; Marcus, R. A. *J. Chem. Phys.* **1985**, *83*, 3462. (b) Wardlaw, D. M.; Marcus, R. A. *J. Phys. Chem.* **1986**, *90*, 5383.
4. Klippenstein, S. J.; Marcus, R. A. *J. Chem. Phys.* **1988**, *92*, 3105.
5. Lee, C. W. *Research Review of Science and Engineering* **1995**, *12*, 221; Ajou University: Suwon, Korea.
6. Clary, D. C. *Mol. Phys.* **1984**, *53*, 3.
7. Keesom, W. H. *Communications from the Physical Laboratory of the University of Leiden*, Supplement No. 24b, p 121-132.
8. Fano, U.; Racah, G. *Irreducible tensorial sets*; Academic: New York, 1959.
9. Edmonds, E. R. *Angular momentum in Quantum Mechanics*; Pricenton: Princeton, 1957.
10. Condon, E. U.; Shortley, G. H. *The Theory of Atomic Spectra*; Cambridge, Cambridge University press, 1935.

Application of Multichannel Quantum Defect Theory to the Triatomic van der Waals Predissociation Process II

Chun-Woo Lee

Department of Chemistry, Ajou University, 5 Wonchun Dong, Suwon 441-749, Korea

Received June 29, 1995

Generalized Multichannel Quantum Defect theory (MQDT) was implemented to the vibrational predissociation of triatomic van der Waals molecules in the previous paper [*Bull. Korean Chem. Soc*, **12**, 228 (1991)]. Implementation was limited to the calculation of the scattering matrix. It is now extended to the calculation of the predissociation spectra and the final rotational distribution of the photofragment. The comparison of the results with those obtained by other methods, such as Golden-rule type calculation, infinite order sudden approximation (IOS), and close-coupling method, shows that the implementation is successful despite the fact that transition dipole moments show more energy dependence than other quantum defect parameters. Examination of the short-range channel basis functions shows that they resemble angle-like functions and provide the validity of the IOS approximation. Besides the validity of the latter, only a few angles are found to play the major role in photodissociation. In addition to the implementation of MQDT, more progress in MQDT itself is made and reported here.

Introduction

Photodissociation provides a wealth of information on molecular dissociation dynamics, as it may be visualized as a half collision process. Traditionally the total dissociation cross sections as functions of the photon energies were measured. However, in an increasing number of recent experiments, final state distributions of the photofragments have been measured. Such experiments were made possible by the availability of powerful light sources and by the development of efficient detection methods like laser induced fluorescence or resonance enhanced multiphoton ionization, and so on. Reliable intermolecular potentials have been deduced from such sophisticated experimental data. Details of photo-

dissociation dynamics are now available for several systems.[1]

However, studies on indirect photodissociation, also called as predissociation, were hampered by lack of computational and interpretative tools. Indirect photodissociation spectra are characterized by their sharp and complicated shapes in contrast to the broad and structureless ones of direct photodissociation spectra. Comparing to the direct photodissociation, indirect photodissociation requires a lot of computational time because scattering equations should be solved for a lot of energy mesh points in order not to miss resonances. Classical trajectory calculations are known to be much much faster than and as equally accurate as close-coupling calculations in direct photodissociation. But they turn out to have problems in use in indirect photodissociation as it is hard for particles to escape once they are captured inside quasi-bound states.

In interpreting the general shapes of the absorption spectra or of final state distributions of the direct processes, reflection principles provide a convenient tool, as greatly emphasized by Schinke.[2] According to reflection principles, the shapes of the dissociation spectra or of the final state distributions reflect the shapes of molecular wavefunctions before light absorption. The reflections are done on the mirrors whose shapes are determined by the "so called" classical excitation functions of conjugate variables to the observables.[3] Such reflection principles can only be applied to direct processes. They can not be applied to indirect processes. Indirect processes pose another problem when the calculations are tried. Classical trajectory method provides a fast-route to calculations for direct processes. It is not an efficient one when indirect processes are involved as particles are hard to escape when they are captured inside the quasi-bound states. Direct close-coupling calculation suffers from the difficulties in finding resonance positions.

On the other hand, a very powerful method, known as multichannel quantum defect theory (MQDT), has been known for a long time in photoionization field.[4] MQDT is now established in atomic physics as one of the most powerful theories unifying treatments on bound and collision state calculations. It provides a unified treatment of bound and continuum wavefunctions by making use of analytic functions that can be analytically continued from bound to continuum regions and vice versa. It also provides the most general theory of resonance phenomena, describing the complicated resonance structures with a small number of energy insensitive parameters. Accordingly, it not only simplifies the task of describing the complicated resonance spectra but also yields great insight into the dynamics of photodissociation or inelastic processes.

In the previous work by the author,[5] MQDT calculation using the generalized MQDT method proposed by Greene, Rau, and Fano[6] was implemented with the replacement of the R-matrix procedure by the close-coupling algorithm. But the implementation was limited to the calculation of the scattering matrix. It is now extended to the calculation of predissociation spectra and final rotational distributions of photofragments. As a model system, van der Waals molecules are chosen, since the computational time is shorter for their system than those of other triatomic molecules because of their weak atom-diatomic interaction potentials. It is also a system for which true state to state measurements of intramolecular energy redistribution are available.

Section 2 gives a brief description of the MQDT theory. Many channel basis functions have been used in MQDT. Since descriptions on them and their relations have not been quite clear or extensive, Section 2 attempts to give more extensive descriptions on them. Section 3 describes the system investigated in this paper. Calculational procedures are described in Section 4. Section 5 summarizes the results.

Theory

Partial photodissociation cross section σ_i for the dissociation channel i is proportional to the frequency of the incident light and to the square of the modulus of the transition dipole moment $\vec{D}^{-(i)}$ given by

$$\vec{D}^{-(i)}=(\Psi^{-(i)}|\vec{\mu}|\Psi_{g'}): \tag{1}$$

$$\sigma_{i}\propto\nu|\vec{D}^{-(i)}|^2. \tag{2}$$

$\Psi^{-(i)}$ denotes the wavefunction of the dissociation channel i satisfying incoming wave boundary conditions and $\vec{\mu}$ is the dipole moment operator. It is known that the dipole moment operator affects the photodissociation dynamics not much for the case of vibrational predissociation of van der Waals molecules and is taken here as a constant. Then the transition dipole moment is approximately proportional to the square of the overlap integral between the initial(normally ground state) and the final wavefunctions. The ground state wave function may be relatively easily obtained from the usual quantum chemical calculations. Final state wavefunctions belonging to the continuum region in case of the photodissociation are obtained by solving scattering equations. Calculations should be done for a lot of energy points as resonance peaks are very sharp and hard to detect accordingly. A lot of energy point calculations are avoided here by making use of multichannel quantum defect theory (MQDT).

MQDT separates the energy sensitive and insensitive parts of calculations which is mostly achieved by simply dividing the coordinate R along which dissociation takes place into inner and outer ranges so that all inelastic processes take place in the inner region. MQDT then utilizes the fact that most time consuming part of traditional close-coupling calculations comes from decoupling the close-coupling equations in the inner region of close-encounter where calculations are insensitive to the scattering energy and need to be done for coarse energy mesh points. Finer energy mesh point calculations are needed only at the outer region where channels are decoupled and the remaining thing to be done is to make wavefunctions satisfy boundary conditions which is much easier than to decouple the close-coupling equations. The equations thus obtained, compatible with the boundary conditions, yield solutions of dynamic quantities which show complicated behaviors and abrupt changes as a function of energy. Such behaviors are caused by the presence of the singularities in the compatibility equations which are caused in turn by the presence of the closed channels.

In MQDT, coordinates R along which fragmentation takes place are divided into two regions $R\leq R_0$ and $R>R_0$. The matching radius R_0 where log derivatives of the solutions at the inner and outer regions coincide, is usually taken so that all inelastic processes are included in the inner re-

gion. In the outer space,motions in the different channel states are decoupled. If standing wave channel basis functions Ψ_i' are considered, their radial wave function defined by $\chi_{ii'}(R)$ for the i channel state Φ_i

$$\Psi_{i'}=\sum_i \Phi_i(\omega)\chi_{ii'}(R), \tag{3}$$

obey the ordinary second order differential equations and are given as linear combinations of regular and irregular solutions:

$$\Psi_{i'}(R,\omega)=\sum_i \Phi_i(\omega)[f_i(R)\delta_{ii'}-g_i(R)K_{ii'}], \quad R\geq R_0 \tag{4}$$

ω denotes collectively all the coordinates but R and $K_{ii'}$ is the real symmetric matrix which differs from the usual K matrix in that its indices i and i' run not only for open but also for closed channels.

The regular and irregular solutions $f_i(R)$ and $g_i(R)$ normalized per unit energy range have the asymptotic forms for the open channels as

$$f_i(R) \rightarrow \left(\frac{2m}{\pi k_i}\right)^{1/2}\sin(k_iR+\eta_i),$$
$$g_i(R) \rightarrow -\left(\frac{2m}{\pi k_i}\right)^{1/2}\cos(k_iR+\eta_i), \tag{5}$$

and for closed channels as

$$f_i(R) \rightarrow \sqrt{\frac{m}{\pi\kappa_i}}\,(\sin\beta_i D_i^{-1}e^{\kappa_iR}-\cos\beta_i D_i\ e^{-\kappa_iR}),$$
$$g_i(R) \rightarrow -\sqrt{\frac{m}{\pi\kappa_i}}\,(\cos\beta_i D_i^{-1}e^{\kappa_iR}+\sin\beta_i D_i\ e^{-\kappa_iR}). \tag{6}$$

Since wavefunctions in the outer region given by Eq. (4) match inner ones at R_0, all the complications of dynamical coupling in the inner region affect the motion of particles in outer region only through the values of K matrix elements. As interaction potentials are highly negative in the inner region, the kinetic energy of the relative motion obtained by subtracting the interacting potentials from photon energies is hardly affected by the relatively small variation of the photon energy as is true in the usual experiments. Thus complicated dynamics occurring in the inner region and accordingly the values of K matrix elements are negligibly affected by the variation of the photon energy.

Though wavefunctions given by Eq. (4) are made to match inner ones at R_0, they do not satisfy the boundary conditions at the asymptotic region. The wavefunctions that satisfy the boundary conditions at the asymptotic region may be obtained by taking linear combinations of the standing wave channel basis functions and then by setting the exponentially rising terms zero. Wave functions then show resonance behavior. It takes much less time to make wave functions satisfy the boundary conditions than to decouple the close-coupling equations and to lessen the burden of fine energy mesh point calculations around sharp resonances accordingly. This design of MQDT makes full use of energy sensitive and insensitive nature of the scattering equations and is much superior to that of the direct method of solving close-coupling equations.

Now let us describe the process of applying the boundary conditions to the linear combinations of Ψ_i'. Here let us follow Fano and introduce "short range" channel basis functions (will be labeled by α) which are just eigenfunctions of the real symmetric K matrix. The eigenvalues of K matrix are conveniently parameterized as $\tan\pi\mu_\alpha$ where μ_α (or $\pi\mu_\alpha$) are called eigenquantum defects (eigenphaseshifts). If we denote the matrix made of eigenvectors of K as U, the form of energy normalized short-range eigenchannel basis functions is given by

$$\Psi_\alpha=\sum_i \Phi_i(\omega)U_{i\alpha}[f_i(R)\cos\pi\mu_\alpha-g_i(R)\sin\pi\mu_\alpha], \tag{7}$$

and their relation with the standing wave channel basis functions Ψ_i is obtained as

$$\Psi_\alpha=\sum_i \Psi_i U_{i\alpha}\ \cos\pi\mu_\alpha. \tag{8}$$

Let us now consider another energy normalized orthogonal channel basisfunctions Ψ_ρ as the superpositions of Ψ_α

$$\Psi_\rho=\sum_\alpha \Psi_\alpha A_{\alpha\rho}, \tag{9}$$

with the coefficients $A_{\alpha\rho}$ so as to satisfy the boundary conditions that the coefficients of the exponentially rising terms are zero at $R\rightarrow\infty$ and that all open channels have the identical phase τ_ρ. Because of the latter condition, Ψ_ρ are eigen channel basis functions at the asymptotic region. Therefore, Ψ_ρ's are eigenfunctions of the ordinary K or S matrix. Substituting Eqs. (5), (6) and (7) into (9) and applying the boundary conditions, the following equations are obtained:

$$\sum_\alpha U_{i\alpha}\sin(\beta_i+\pi\mu_\alpha)A_{\alpha\rho}=0, \quad i \in \text{closed} \tag{10}$$

$$\sum_\alpha U_{i\alpha}\cos\pi\mu_\alpha A_{\alpha\rho}=T_{i\rho}\cos\pi\tau_\rho,$$
$$\sum_\alpha U_{i\alpha}\sin\pi\mu_\alpha A_{\alpha\rho}=T_{i\rho}\sin\pi\tau_\rho, \quad i \in \text{open} \tag{11}$$

Above equations can be transformed into the generalized eigenvalue equations

$$\sum_\alpha \Gamma_{i\alpha}A_{\alpha\rho}=\tan\pi\tau_\rho\sum_\alpha \Lambda_{i\alpha}A_{\alpha\rho}, \tag{12}$$

with their matrix elements

$$\Gamma_{i\alpha}=\begin{cases} U_{i\alpha}\sin(\beta_i+\pi\mu_\alpha), & i \in \text{closed channel,} \\ U_{i\alpha}\sin\pi\mu_\alpha, & i \in \text{open channel,} \end{cases} \tag{13}$$

$$\Lambda_{i\alpha}=\begin{cases} 0, & i \in \text{closed channel,} \\ U_{i\alpha}\cos\pi\mu_\alpha, & i \in \text{open channel.} \end{cases} \tag{14}$$

As described above, the time required to solve Eq. (12) for detecting resonances is much shorter than to solve close-coupling equations. We also note that by the above procedure of MQDT, five energy-insensitive parameters η_i, D_i, μ_α, and $U_{i\alpha}$ in Eq. (5), (6) and (7) are disentangled as the only parameters needed to describe the complicated resonance phenomena. [With one more parameter, transition dipole matrix elements $D_\alpha=(\Psi_{gr}||\vec{\mu}||\Psi_\alpha)$ in case of photodissociation cross sections]. In the semiempirical application of MQDT, short-range parameters μ_α and frame transformation matrix U are usually assumed a constant function of energy. The energy dependence of the remaining parameters η_i and β_i is known analytically in case of Coulombic and dipole (attractive) field cases but should be obtained numerically for zero field case.

Now wavefunctions satisfying the appropriate boundary conditions can be obtained as a superposition of energy normalized Ψ_ρ. For example, $\Psi^{-(i)}$ satisfying the incoming wave

boundary conditions are given as

$$\Psi^{-(i)}=\sum_{\rho}C_{\rho}{}^{-(i)}\Psi_{\rho}, \tag{15}$$

with

$$C_{\rho}{}^{-(i)}=i(T^{-1})_{\rho i}\ e^{-i(\eta_i+\pi c_\rho)}. \tag{16}$$

Since $T_{i\rho}$ is orthogonal, $C_{\rho}{}^{-(i)}$ is unitary.

Or, equivalently, it could be given in term of short range channel basis functions by

$$\Psi^{-(i)}=\sum_{\alpha}A_{\alpha}{}^{-(i)}\Psi_{\alpha}, \tag{17}$$

with

$$A_{\alpha}{}^{-(i)}=ie^{-i\eta_i}\sum_{\beta}U_{i\beta}e^{i\pi c_\beta}\sum_{\rho}A_{\alpha\rho}A_{\beta\rho} \tag{18}$$

When all the channels are open, solutions of (12) can be obtained analytically and are given by

$$A_{\alpha\rho}=e^{-i\pi\mu_\alpha}\sum_{i}U_{\alpha i}{}^{\dagger}T_{i\rho}e^{i\pi c_\rho}, \text{ (when all channels open)}, \tag{19}$$

and satisfy orthogonality relation

$$\sum_{\rho}A_{\alpha\rho}A_{\beta\rho}=\delta_{\alpha\beta} \text{ (when all channels open)}. \tag{20}$$

If $\bar{A}_{\alpha}{}^{-(i)}$ denote $A_{\alpha}{}^{-(i)}$ of Eq. (17) when all the channels open, they are given by

$$\bar{A}_{\alpha}{}^{-(i)}=ie^{-i\eta_i}U_{i\alpha}e^{-i\pi\mu_\alpha} \tag{21}$$

and orthogonal to each other

$$\sum_{\alpha}\bar{A}_{\alpha}{}^{-(i)}\bar{A}_{\beta}{}^{-(j)}=\delta_{ij}. \tag{22}$$

Using $\bar{A}_{\alpha}{}^{-(i)}$, $A_{\alpha}{}^{-(i)}$ may be expanded as

$$A_{\alpha}{}^{-(i)}=\sum_{j}C_{ij}\bar{A}_{\alpha}{}^{-(j)} \tag{23}$$

where the expansion coefficients are given by

$$C_{ij}=\sum_{\rho}\Big(\sum_{\alpha}\bar{A}_{\alpha}{}^{-(i)*}A_{\alpha\rho}\Big)\Big(\sum_{\beta}\bar{A}_{\beta}{}^{-(j)}A_{\beta\rho}\Big). \tag{24}$$

Notice that i belongs to open channels as evident from Eq. (17) while j could belong to closed as well as open ones. If we substitute Eq. (21) into Eq. (11), we obtain

$$\sum_{\alpha}\bar{A}_{\alpha}{}^{-(i)*}A_{\alpha\rho}=-ie^{i\eta_i}T_{i\rho}\ e^{i\pi c_\rho},\ i\in \text{open} \tag{25}$$

By substituting the above equations into Eq. (24),

$$C_{ij}=\sum_{\rho}T_{i\rho}T_{j\rho}. \tag{26}$$

It is well known that $T_{i\rho}$ is an orthogonal real matrix. Then C_{ij} becomes δ_{ij} when j is open (as we said above, i belongs to open channels). If j is closed, C_{ij} is given by

$$C_{ij}=\sum_{\beta\gamma}\bar{A}_{\beta}{}^{-(j)*}\Delta_{\beta\gamma}\bar{A}_{\gamma}{}^{-(i)} \tag{27}$$

where $\Delta_{\beta\gamma}$ is defined as

$$\Delta_{\beta\gamma}=\sum_{\rho}A_{\beta\rho}A_{\gamma\rho}. \tag{28}$$

At off resonances, $\Delta_{\beta\gamma}$ becomes $\delta_{\beta\gamma}$ for β and γ belonging to open channels according to Eq. (20) and zero for β and γ belonging to closed channels. The latter holds in the following reason. At off-resonance, Eq. (10) and Eq. (11) are decoupled and $A_{\alpha\rho}$, for $\alpha\in$ closed, may be obtained with Eq. (10) alone. $\sin(\beta_i+\mu_\alpha)$ are far from zero at off-resonance and therefore the only sure way for Eq. (10) to hold is for $A_{\alpha\rho}$ to be zero.

Overall, $A_{\alpha}{}^{-(i)}$ can be expanded into the orthogonal vectors $\bar{A}_{\alpha}{}^{-(i)}$ as

$$\begin{aligned}A_{\alpha}{}^{-(i)}&=\bar{A}_{\alpha}{}^{-(i)}+\sum_{j\in\text{closed}}\bar{A}_{\alpha}{}^{-(j)}\sum_{\beta\gamma}\bar{A}_{\beta}{}^{-(j)*}\Delta_{\beta\gamma}\bar{A}_{\gamma}{}^{-(i)}\\&=\bar{A}_{\alpha}{}^{-(i)}+\sum_{j\in\text{closed}}\bar{A}_{\alpha}{}^{-(j)}\langle\Psi^{-(j)}|\Delta|\Psi^{-(i)}\rangle\equiv\bar{A}_{\alpha}{}^{-(i)}\\&\quad+\sum_{j\in\text{closed}}\bar{A}_{\alpha}{}^{-(j)}\bar{\Delta}_{ji}.\end{aligned} \tag{29}$$

$\bar{\Delta}_{ji}$ may be considered as the matrix elements of Δ in the basis set of $|\Psi^{-(i)}|$ and have the following form:

$$\bar{\Delta}_{ij}=\sum_{\beta}\bar{A}_{\beta}{}^{-(j)*}A_{\beta}{}^{-(i)} \tag{30}$$

$$=\sum_{\rho}\Big(\sum_{\beta}\bar{A}_{\beta}{}^{-(j)*}A_{\beta\rho}\Big)C_{\rho}{}^{-(i)}, \tag{31}$$

The above equation shows us the effect of closed channels to the photodissociation. $\bar{\Delta}_{ji}$ may be considered as the coupling strength between the closed channel j and the open channels i. (We may consider $\bar{A}_{\alpha}{}^{-(i)}$ as the frame transformation matrix between short range channels $|\alpha\rangle$ and the incoming wave channels $|i\rangle$ while $U_{i\alpha}$ as the one between $|\alpha\rangle$ and the standing wave channels $|i\rangle$.) If j belongs to open channels, it is easy to show that $\bar{\Delta}_{ij}$ becomes δ_{ij}.

If we consider two channel case where one channel is open and another closed, analytical solutions for $\Delta_{\beta\gamma}$ may be obtained and $A_{\alpha}{}^{-(i)}$ becomes

$$A_{\alpha}{}^{-(1)}=\bar{A}_{\alpha}{}^{-(1)}-e^{i(\eta_2-\eta_1)}e^{-i(\beta+\pi c)}\Big(\pi\frac{d\tau}{d\beta}\Big)^{1/2}\bar{A}_{\alpha}{}^{-(2)} \tag{32}$$

where $\pi\dfrac{d\tau}{d\beta}$ can be expanded as

$$\pi\frac{d\tau}{d\beta}=\pi\frac{d\tau}{dE}\ \frac{dE}{d\beta}=\frac{t_D}{2\hbar}\ \frac{dE}{d\beta} \tag{33}$$

around resonance. t_D is the time delayed by resonance and thus expected to be always positive and shows the resonance behaviors. Also for two channel case, we notice that

$$tr\Delta=\sum_{\alpha}A_{\alpha}{}^{2}=1+\pi\frac{d\tau}{d\beta}. \tag{34}$$

Numerical studies show that the above properties of Δ hold for more than two channel cases, though analytical solutions such as the above are not available yet.

Let us summarize channel basis functions and their relations described so far. First, Table 3 shows all the channel basis and their asymptotic or decoupled forms. The table also shows whether they are energy normalized, whether closed channels are included in channel couplings. Figure 1 diagrammatically shows where they are defined, and what are their characteristics. Are they defined in the asymptotic region or in the short-range region? Are they standing waves, incoming waves, or eigenchannels? It also exhibits various frame transformation matrices that connect two of them. Analytical forms of frame transformation matrices are

Table 1. Parameters for the model intermolecular system A-B_2

(a) Reduced mass between A and B_2	
m=6756.8a.u.	
(b) Morse potential parameter	
D_{AB}=0.0034 eV	D_{CM}=0.00195 eV
α_{AB}=1.0 a.u.	α_{CM}=1.0 a.u.$^{-1}$
$R_{AB}^{(e)}$=6.82 a.u.	$R_{CM}^{(e)}$=6.65 a.u.
(c) van der Waals potential parameter	
C_{60}=0.75 eV (a.u.)$^{-6}$	
C_{62}=0.119 eV (a.u.)$^{-6}$	
C_{80}=1.58 eV (a.u.)$^{-8}$	
C_{82}=0.8 eV (a.u.)$^{-8}$	

Table 2. Diatomic molecular parameters

vibrational frequency	ω_e	0.0162 eV
rotational constant	B	0.01758 meV
equilibrium bond length	r_e	3.044 a.u.
reduced mass	μ	32576.6 a.u.

Table 3. Various channel basis functions used in MQDT

basis functions	energy normalized	channels involved	decoupled or asymptotic form
$\Psi_{i'}$	no	open, closed	$\sum_i \Phi_i(\omega)[f_i(R)\delta_{ii'}-g_i(R)K_{ii'}]$
Ψ_α	yes	open, closed	$\sum_i \Phi_i(\omega)U_{i\alpha}[f_i(R)\cos\pi\mu_\alpha - g_i(R)\sin\pi\mu_\alpha]$
Ψ_ρ	yes	open	$\sum_i \Phi_i(\omega)T_{i\rho}[f_i(R)\cos\pi\tau_\rho - g_i(R)\sin\pi\tau_\rho]$
$\Psi^{-(i)}$	yes	open	$\sum_i \Phi_i(\omega)\sqrt{m/2\pi\kappa_i}[e^{ik_iR}\delta_{ii'} - e^{ik_iR}S_{ii'}]$
$\Psi^{(i')}$	no	open	$\sum_i \Phi_i(\omega)[f_i(R)\delta_{ii'}-g_i(R)K_{ii'}]$

summarized in Table 4. The table also shows their forms when all the channels open, and whether they are unitary or not. Relations among various frame transformation matrices are shown in Table 5. The complexity of the relations arises from the fact that some frame transformation matrices are not unitary as shown in Table 4.

So far, we described how to obtain final state wavefunctions $\Psi^{-(i)}$ by MQDT. In MQDT, they are expressed in terms of short-range channel basis functions Ψ_α by Eq. (17). Then, transition dipolemoment $D^{-(i)}$ may be expanded into

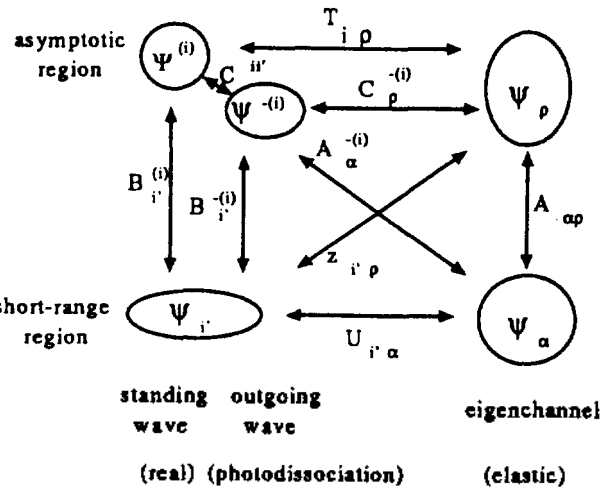

Figure 1. Diagrams showing the relations among various channel basis functions.

Table 4. Various frame transformation matrices. $z_{i\rho}$ is defined as $\Psi_\rho=\sum_\rho \Psi_i z_{i\rho}\cos\pi\tau_\rho$. $B_{i'}^{\ i}$ is defined as $\Psi^{(i)}=\sum_{i'}\Psi_{i'}B_{i'}^{\ i}$

	unitarity	analytical form or definition		all channels open
$U_{i\alpha}$	yes	$K_{ii'}=\sum_\alpha U_{i\alpha}\tan\pi\mu_\alpha U_{\alpha i'}^{\dagger}$		$U_{i\alpha}$
$A_{i\rho}$	no	$[U^{\dagger}z]_{\alpha\rho}\cos\pi\tau_\rho/\cos\pi\mu_\alpha$		$\delta_{\alpha\rho}$
$T_{i\rho}$	yes	$K_{ii'}=\sum_\rho T_{i\rho}\tan\pi\tau_\rho T_{\rho i'}^{\dagger}$		$U_{i\alpha}\delta_{\alpha\rho}$
$C_\rho^{-(i)}$	yes	$ie^{-i\eta_i}T_{i\rho}e^{-i\pi\tau_\rho}=\sum_\alpha \bar{A}_\alpha^{-(i)}A_{\alpha\rho}$		$ie^{-i\eta_i}U_{i\alpha}e^{-i\pi\mu_\alpha}\delta_{\alpha\rho}$
$A_\alpha^{-(i)}$	no	$ie^{-i\eta_i}\sum_\beta U_{i\beta}e^{-i\pi\mu\beta}\Delta_{\beta\alpha}$ $=\bar{A}_\alpha^{-(i)}+\sum_{i\in\text{closed}}\bar{A}_\alpha^{-(i)}\Delta_{ii}^{-}$		$ie^{-i\eta_i}U_{i\alpha}e^{-i\pi\mu_\alpha}$
$z_{i\rho}$	no	$\begin{cases} T_{i\rho}, & i\in\text{open} \\ -[(\tan\beta+K)^{-1}KT]_{i\rho}, & i\in\text{closed} \end{cases}$		$U_{i\alpha}\cos\pi\mu_\alpha\delta_{\alpha\rho}$
$B_{i'}^{\ i}$	no	$\begin{cases} \delta_{ii'}, & i'\in\text{open} \\ -[(\tan\beta+K)^{-1}K]_{ii'}, & i'\in\text{closed} \end{cases}$		$\delta_{ii'}$

$$D^{-(i)}=\sum_\alpha A_\alpha^{-(i)*}D_\alpha=-ie_i^{i\eta_i}\sum_\alpha B_{i\alpha}D_\alpha \tag{35}$$

where $B_{i\alpha}$ is given by

$$B_{i\alpha}=\sum_\beta U_{i\beta}\ e^{i\pi\mu_\alpha}\Delta_{\alpha\beta}, \tag{36}$$

System

Here we consider the system of vibrational predissociations of triatomic van der Waals molecules, identical to one

Table 5. Relations among transformations between frames at asymptotic region and at short-range region. $B_{i'}^{\ -(i)}$ is defined as $\Psi^{-(i)}=\sum_{i'}\Psi_{i'}B_{i'}^{\ -(i)}$

	$A_{\alpha\rho}$	$A_\alpha^{-(i)}$	$z_{i\rho}$	$B_{i'}^{-(i)}$	$B_{i'}^{(i)}$
$A_{\alpha\rho}$	1	$\sum_i A_\alpha^{-(i)}C_\rho^{-(i)*}$	$\sum_i U_{\alpha i}^{\dagger}z_{i\rho}(\cos\pi\tau_\rho/\cos\pi\mu_\alpha)$	–	–
$A_\alpha^{-(i)}$	$\sum_\rho A_{\alpha\rho}C_\rho^{-(i)}$	1	–	$\sum_{i'}U_{\alpha i'}^{\dagger}B_{i'}^{-(i)}$	–
$Z_{i\rho}$	$\sum_\alpha U_{i\alpha}(\cos\pi\mu_\alpha/\cos\pi\tau_\rho)A_{\alpha\rho}$	–	1	–	$\sum_{i'}B_i^{(i')}T_{i'\rho}$
$B_{i'}^{-(i)}$	–	$\sum_\alpha U_{i'\alpha}\cos\pi\mu_\alpha A_\alpha^{-(i)}$	$\sum_\rho z_{i'\rho}\cos\pi\tau_\rho C_\rho^{-(i)}$	1	–
$B_i^{(i)}$	–	$\sum_\alpha U_{i'\alpha}\cos\pi\mu_\alpha A_\alpha^{(i)}$	$\sum_\rho z_{i'\rho}\cos\pi\tau_\rho T_{\rho i}^{-1}$	–	1

of the author's previous work.[5] Triatomic van der Waals molecules are restricted to rare gas-homonuclear halogen diatomic molecules. Empirical potentials for them like $NeCl_2$, $HeCl_2$[7] are well established owing to the state-to-state measurements available for them. The interaction potential between A and B_2 in AB_2 triatomic system used by Halberstadt *et al.*[8] for $NeCl_2$ system has the following form (a slightly modified form for $HeCl_2$)

$$V(R, r, \gamma)=V_M(R, r, \gamma), \quad \text{when } R\le R^*,$$
$$V(R, r, \gamma)=V_{vdW}(r, \gamma)+(V_M-V_{vdW})e^{-\alpha(R-R^*/R^*)^2}, \quad \text{when } R\ge R^*, \tag{37}$$

in the Jacobi coordinates R, r, γ that denote the distance between A and the center of mass of B_2, the bond distance of B_2, and the angle between $\vec{R}$ and $\vec{r}$, respectively. $V_M(R, r, \gamma)$ and V_{vdW} are given as

$$V_M(R, r, \gamma)=D_{AB}\sum_{i=1}^{2}\{[e^{-\alpha_{AB}(R_{AB_i}-R_{AB}^{(e)})}-1]^2-1\}^2 \tag{38}$$

$$+D_{CM}\{[e^{-\alpha_{CM}(R-R_{CM}^{(e)})}-1]^2-1\}^2, \tag{39}$$

$$V_{vdW}(R, \gamma)=-\frac{C_6(\gamma)}{R^6}-\frac{C_8(\gamma)}{R^8}, \tag{40}$$

where R_{AB_i} is the distance between A and i^{th} B atom, R is same as above, and other parameters are constant that are adjusted to yield the best fit to the experimental values. Two Legendre terms are retained for $C_6(\gamma)$ and $C_8(\gamma)$, e.g.,

$$C_6(\gamma)=C_{60}+C_{62}P_2(\cos\gamma). \tag{41}$$

R^* is chosen as the inflection point of the atom-atom Morse potentials and given by $R^*=R_{CM}^{(e)}+\ln 2/\alpha_{CM}$. The parameters used in this paper are slightly different from those of Ref. 8 and given in Table 1.

With this interaction potential, the Hamiltonian for the triatomic van der Waals molecules AB_2 is given in the Jacobi coordinates by[9]

$$H=-\frac{1}{2m}\frac{\partial^2}{\partial R^2}+\frac{\vec{j}^2}{2\mu r^2}+\frac{\vec{l}^2}{2mR^2}+V(R, r, \gamma)+H_{B_2}(r), \tag{42}$$

with

$$H_{B_2}(r)=-\frac{1}{2\mu r^2}\frac{\partial^2}{\partial r^2}+V_{B_2}(r), \tag{43}$$

that denotes the vibrational Hamiltonian of B_2. m and μ denote the reduced mass of A and the center of mass of B_2 and of B_2, respectively; $\vec{j}$, the angular momentum operator of B_2; and $\vec{l}$, the orbital angular momentum operator of the relative motion of A and the center of mass of B_2. The values used for B_2 are in Table 2.

The values of total angular momentum operator $\vec{J}=\vec{j}+\vec{l}$, as is well known both experimentally and theoretically, do not affect the predissociation dynamics much and is set to zero hereafter. This simplifies the Hamiltonian as $\vec{l}$ can be set to equal to $\vec{j}$.

When the wavefunctions $\Psi^{-(i)}(R, r, \gamma)$ to the dissociation channel $i=\{vj\}$ are expanded in base functions $\Phi_{i'}(r, \gamma)=(r|v')Y_{j'0}(\gamma, 0)$ for the rovibrational channel $i'=\{v'j'\}$ as

$$\Psi_i(R, r, \gamma)=\sum_{i'}\Phi_{i'}(r, \gamma)\chi_{i'i}(R), \tag{44}$$

the close-coupling equations are given as

$$\left[-\frac{1}{2m}\frac{d^2}{dR^2}-k_{i'}^2+\frac{j^2}{2mR^2}\right]\chi_{i'i}(R)+\sum_{i''}V_{i'i''}(R)\chi_{i''i}(R)=0, \tag{45}$$

with

$$k_i^2=2m[E-Bj(j+1)-(v+\frac{1}{2})\omega], \tag{46}$$

and

$$V_{i'i''}(R)=\int d\gamma\sin\gamma\int dr\Phi_{i'}(r, \gamma)V(R, r, \gamma)\Phi_{i''}^*(r, \gamma). \tag{47}$$

In the practical calculations of $V_{i'i''}(R)$, the interaction potential is expanded into Legendre polynomials and then the angle integration is performed analytically to yield the formula in terms of $3j$ symbols.

The real symmetric K matrix in (4) is easily obtained by simply replacing $\exp(\pm ik_iR)$ or $\sin k_iR$ and $\cos k_iR$ in the conventional close-coupling computer code with the energy normalized base pair $f_i(R)$ and $g_i(R)$. The important difference between the close-coupling and the K matrix calculation is that the subindex i includes both open and closed channels for the latter while it includes only open channels for the former.

Calculation

In MQDT, a transition dipole moment to channel i given by Eq. (35). D_α is the transition dipole moment to the short range channel α and is expected to be insensitive to energy. The abrupt change of $D^{-(i)}$ as a function of energy, then, derives from $A_\alpha^{-(i)}$. D_α is defined as the integral $(\Psi_\alpha|\mu|\Psi_{gr})$. The ground state wavefunction is simply assumed to be Gaussian functions of R and γ here since the purpose of this work is in implementing MQDT to photodissociation, and not in calculating the transition dipole moment as exactly as possible.

$$\Psi_{gr}(R, r, \gamma)=\frac{1}{2}\{\exp[-a_R(R-R_e)^2]+\exp[-a_R(R+R_e)^2]\}$$
$$\times\exp[-a_\gamma(\gamma-\gamma_e)^2]\langle r|n=0\rangle$$
$$\equiv\Phi_R(R)\Phi_\gamma(\gamma)\langle r|n=0\rangle \tag{48}$$

$\Phi_\gamma(\gamma)$ is expanded into the spherical harmonics in order to utilize the latter's orthonormal property for integrating over γ:

$$\Phi_\gamma(\gamma)=\sum_j a_jY_{j0}(\gamma, 0) \tag{49}$$

In order to obtain Ψ_α, the close-coupling equations (45) are solved from $R=0$ to $R=R_0$ and their solutions are linearly combined to make the boundary conditions given by Eq. (4) satisfied. Then Ψ_α are obtained as eigenvectors of the K matrix. In order to apply the boundary conditions (4), a regular and irregular base pair in $R>R_0$ should be prepared at first. The pair may be obtained analytically for Coulomb and dipole fields, but should be calculated numerically for the zero field (where potential decreases faster than $1/R^2$ as a function of R). The present system belongs to the zero field case since the long-range part of the intermolecular potential of the present van der Waals system decreases as

$1/R^6$ as in Eq. (40). Though the regular and irregular base pair is defined only at the range of $R>R_0$, its calculation needs to start from $R=0$, since the regularity of the solution is determined by its behavior at the origin. In order to calculate it at $R<R_0$, the decoupled potentials at $R>R_0$ needs to be extrapolated to $R<R_0$ where they are not decoupled. Actually the detailed forms of the potentials at $R<R_0$ should not be important, because the base pairs have no meaning there. Let us call the arbitrarily extrapolated potential a reference potential. The choice of the reference potential should not affect the final result but changes the values of quantum defect parameters (qdt) η and β. Two extrapolations using adiabatic and diabatic potentials may be well defined and can be utilized for any system without arbitrariness as reference potentials. Diabatic and adiabatic potentials connected to $\{vj\}$ fragmentation channels are defined as

$$V_{\text{diab}}^{vj}(R)=V_{vj,vj}(R)+\frac{j(j+1)}{2mR^2}+Bj(j+1)+(v+\frac{1}{2})\omega$$

$$V_{\text{adiab}}^{vj}(R)=v_{vj}(R)+\frac{j(j+1)}{2mR^2}+Bj(j+1)+(v+\frac{1}{2})\omega \quad (50)$$

where $v_{vj}(R)$ are the eigenvalues of the hermitian matrix $V_{vj,v'j'}(R)$. However, for the system of interest, these extrapolations can not be applied since the reference potentials from these extrapolations may have potential minimum higher than the predissociation resonance energies. As particles with negative kinetic energy in all space can not exist, $f_i(R)$ and $g_i(R)$ pair cannot be defined under such reference potentials. But the presence of resonance energies indicates that particles can still have positive kinetic energies in such resonance energies. The drawback of the above potentials is that they are averaged over angles. The potential minimum along the trough of $V(R, r, \gamma=90°)$ is lower than the resonance energies as it should be. The reference potential V_{ref} can thus be taken as:

$$V_{\text{ref}}(R)=\begin{cases}V_{\text{IOS}}(R), & R\le R^*,\\ V_{\text{diab}}^{vj}(R)+(V_{\text{IOS}}-V_{\text{diab}}^{vj})e^{-\rho(R-R^*/R^*)}, & R\ge R^*,\end{cases} \quad (51)$$

with

$$V_{\text{IOS}}(R)\equiv(R, r_e, \gamma_e)+\frac{j(j+1)}{2mR^2}+Bj(j+1)+(v+\frac{1}{2})\hbar\omega. \quad (52)$$

ρ is chosen to ensure the smooth connection at $R=R^*(R^*=4$ Å and $\rho=25$ are used).

Once reference potentials are chosen, the base pair $f_i(R)$ and $g_i(R)$ can be obtained by solving the ordinary differential equations which are obtained from (45) by extrapolating the decoupled $V_{vj,v'j'}(R)$ (identical to $v_{vj}(R)$ at $R>R_0$) to the reference potentials at $R<R_0$ [see Eq. (50)]. Their calculation in MQDT may cause trouble in two respects. First, irregular solutions $g_i(R)$ are singular at the origin. Second, MQDT requires them not only at the positive energies but also at the negative energies where the base pair is singular.

Milne method recommended in Ref. 6 is shown to be stable enough even in the deeply classically forbidden region to overcome these difficulties. This stability derives from the fact that it calculates the more slowly varying functions of R, that is, amplitudes and phases of the regular and irregular functions than the wavefunctions themselves.

In the Milne procedure, the base pair is replaced with $\alpha_i(R)$ and $\phi_i(R)$ by the transformation

$$f_i(R)=\sqrt{\frac{2}{\pi}}\alpha_i(R)\sin\phi_i(R),$$

$$g_i(R)=-\sqrt{\frac{2}{\pi}}\alpha_i(R)\cos\phi_i(R). \quad (53)$$

for both positive and negative energies.

$\phi_i(R)$ is given in terms of α_i by

$$\phi_i(R)=\int_0^R \alpha_i^{-2}(R')dR'. \quad (54)$$

The function α itself satisfies the ordinary second order differential equations

$$\frac{d^2\alpha_i(R)}{dR^2}+k_i^2(R)\alpha_i(R)=\alpha_i^{-3}(R), \quad (55)$$

with

$$k_i^2(R)=2m[E-V_{\text{ref}}(R)]. \quad (56)$$

The boundary conditions for $\alpha_i(R)$ are chosen so as to make the variation of $\alpha_i(R)$ as a function of R as small as possible, as it leads to the minimization of the numerical error. At the positive energies, such boundary conditions are obtained as

$$\alpha_i(R)\to k_i^{-1/2}, \quad \frac{d\alpha_i(R)}{dR}\to\frac{dk_i(R)^{-1/2}}{dR}=0, \text{ at } R\to\infty \quad (57)$$

At the negative energies, applying the same kind of boundary conditions at the potential minimum instead of at the asymptotic region, namely

$$\alpha_i(R_c)\to k_i^{-1/2}, \quad \frac{d\alpha_i(R_c)}{dR}\to 0 \quad (58)$$

has been proposed as a means of reducing the oscillations in $\alpha_i(R)$ and $\phi_i(R)$ as much as possible. The quantum defect parameter β_i is identified in the Milne procedure as

$$\beta_i\equiv\int_0^\infty \alpha_i(R)^{-2}dR. \quad (59)$$

The second order equation (55) and the close-coupling equation (45) are solved by the De Vogelaere algorithm[10] which is particularly suitable for the integration of (59) by a Simpson formula, since it generates $\alpha_i(R)$ not only at the propagation mesh points but also at their middle points.

With the solutions $\chi_{j'}^{n'(i)}$ of close-coupling equation (45) and the regular and irregular base pair $f_i(R)$ and $g_i(R)$ obtained by Milne method, short-range channel basis functions are given with the explicit vib-rotational quantum number notations of i and i' by

$$\Psi_\alpha=\begin{cases}\sum_{nj}\Psi_{nj}U_{nj,\alpha}\cos\pi\mu_\alpha\\ \sum_{n'j'}[\langle r|n'\rangle Y_{j'0}(\gamma, 0)\sum_{nj}\chi_{n'j',nj}(R)U_{nj,\alpha}\cos\pi\mu_\alpha], & \text{when } R<R_0,\\ \sum_{n'j'}\langle r|n'\rangle Y_{j'0}(\gamma, 0)U_{n'j',\alpha}[f_{n'j'}(R)\cos\pi\mu_\alpha\\ \quad -g_{n'j'}(r)\sin\pi\mu_\alpha], & \text{when } R>R_0.\end{cases} \quad (60)$$

Then D_α is calculated by

$$D_\alpha=(\Psi_\alpha|\mu|\Psi_{gr})\propto\sum_{nj}U_{nj,\alpha}\cos\pi\mu_\alpha\sum_{n''j''}\langle n'|\mu|n''\rangle a_j$$
$$\times\left\{\int_0^{R_0}\chi_{nj,n'j'}(R)\Phi_R(R)dR\right.$$
$$\left.+\int_{R_0}^{\infty}[f_{nj}(R)\cos\pi\mu_\alpha-g_{nj}(R)\sin\pi\mu_\alpha]\Phi_R(R)dR\right\} \quad (61)$$

where n'' is the vibrational quantum number of the ground state. The value of $\langle n'|\mu|n''\rangle$ is taken arbitrarily.

In order to calculate transition dipole moment $D^{-(i)}$, in addition to D_α we need $\bar{A}_\alpha{}^{-(i)}$ or $B_{i\alpha}$ which are in turn obtained by solving MQDT Equations (12). The equations are the generalized eigenvalue equations of the form $Ax=\lambda Bx$, and are solved by so called QZ algorithm which is equivalent to the QR algorithm of $B^{-1}A$ but the inverse of B is never explicitly calculated. QZ algorithm is especially useful to our problem since B, denoted as Λ here, is singular and its inverse can not be calculated.[11] Λ is singular since the rows corresponding to closed channels are zero. The code in C for the generalized eigenvalue equation was not available and was written by converting a Fortran code.

Though solving MQDT equations is not much time consuming, it is still very annoying to solve it for a broad energy range since we have to change the magnitudes of intervals around resonances in order not to miss them and to make smooth spectra around resonances. In order to avoid this inconveniences, we adapt the variable step sizes in energy variation. If the maximum variations of τ_ρ in the next energy mesh point are smaller than some value, we increase the energy step size by some value, say 1.4. If τ_ρ vary too much in one step move, we decrease the step size by half and do not accept the new τ_ρ and other quantities at that energy mesh point. Such values are not discarded but are stored in a stack for later steps. Keeping the size of variations of τ_ρ for each step smaller than some value is not sufficient to ensure the smooth variation of τ_ρ at each step. In order to ensure the smooth variation of τ_ρ at each step, we have to discard the energy point if the first derivatives of τ_ρ with respect to E vary too rapidly. All these points are implemented in the computer code.

Results of MQDT calculations are compared with those of three other methods, namely, close coupling calculation, Golden-rule type calculation and infinite order sudden calculation (IOS). As in MQDT calculation, close coupling calculation is performed by De Vogelaere algorithm.[10]

In Golden-rule type calculation, the resonance life time is obtained by[12]

$$2\pi|(\phi_b|V(R,\ r,\ \gamma)|\Psi_c{}^{-(i)})|^2. \quad (62)$$

ϕ_b and $\Psi_c{}^{-(i)}$ denote the quasi bound and continuum states, respectively, and are obtained by including close channels alone for the former and open ones alone for the latter in solving close coupling equations. $\Psi_c{}^{-(i)}$ may be obtained by the usual close-coupling algorithm, namely considering n independent solutions satisfying the boundary conditions at the origin $R=R_i$, $\Psi_{cj'}{}^{-(i)}(R_i)=0$, $d\Psi_{cj'}{}^{-(i)}/dR=\delta_{ii'}$, $(j=1,2,\cdots,n)$ and propagating them to $R=R_0$ and applying the following boundary conditions

$$\sum_j\Psi_{cj'}{}^{-(i)}A_{jj''}=\sum_j\sqrt{\frac{2m_{j'}}{\pi k_{j'}}}[e^{ik_{j'}R}\delta_{j'j''}-e^{-ik_{j'}R}S_{j'j''}]$$

$$\sum_j\frac{d\Psi_{cj'}{}^{-(i)}}{dR}A_{jj''}=i\sum_j\sqrt{\frac{2m_{j'}k_{j'}}{\pi}}[e^{ik_{j'}R}\delta_{j'j''}+e^{-ik_{j'}R}S_{j'j''}]. \quad (63)$$

Such algorithm may not be applied to obtain ϕ_b for which all the channels are closed and small errors in propagating the solutions may be exponentially amplified in the classically forbidden region. In this case, we solve close-coupling equation by starting at both ends, $R=R_i$ and $R=R_f$ and then propagating the solutions toward the matching radius $R=R_0$. Two solutions are linearly transformed so that they and their first derivatives are matched at $R=R_0$. Let us denote two solutions by ϕ_a and ϕ_b and two linear transformations by A and B. Then

$$A\phi_a=B\phi_b$$
$$A\frac{d\phi_a}{dR}=B\frac{d\phi_b}{dR}. \quad (64)$$

In the real problem, quasi-bound states are obtained by including only $n=1$ vibrational quantum states and continuum states by including only $n=0$ vibrational ones. They may be expressed as

$$\phi_b=\sum_j(P_{bj})^{1/2}\chi_{bj}(R)Y_{j0}(\gamma,\ 0)\langle r|1\rangle \quad (65)$$

and

$$\Psi_c{}^{-(i)}(R)=\sum_j\chi_{cj'}{}^{-(i)}(R)Y_{j'0}(\gamma,\ 0)\langle r|0\rangle \quad (66)$$

where $\chi_{bj}(R)$ is taken to be normalized with respect to the integration over R, *i.e.*

$$\int_0^\infty|\chi_{bj}(R)|^2dR \quad (67)$$

and P_{bj} are the probabilities for the bound state to be in the rotational state j. If the intermolecular potential is expanded up to the first terms of $(r-r_e)$ *i.e.*

$$V(R,\ r,\ \gamma)=V_0(R,\ \gamma)+V_1(r,\ \gamma)\ (r-r_e) \quad (68)$$

and each V_0 and V_1 terms are expanded in terms of harmonics as

$$V(R,\ r,\ \gamma)=\sum_k V_{0k}(R)P_k(\cos\gamma)+\sum_k V_{1k}(R)P_k(\cos\gamma)(r-r_e), \quad (69)$$

then the probability amplitude to the dissociation state j can be rewritten as

$$V_{bc}(j)=(\phi_b|V|\Psi_c{}^{-(i)})$$
$$=\langle 1|r-r_e|0\rangle\sum_{kj'j''}(Y_{j'0}|P_k|Y_{j''0})(\chi_{bj'}|V_{1k}|\chi_{cj''}{}^{-(i)})$$
$$=\frac{1}{\sqrt{2m\omega}}\sum_{j'j''}[(2j'+1)(2j''+1)]^{1/2}\sum_k\begin{pmatrix} j' & j'' & k\\ 0 & 0 & 0\end{pmatrix}^2$$
$$(\chi_{bj'}|V_{1k}|\chi_{cj''}{}^{-(i)}). \quad (70)$$

In the infinite order sudden approximation (IOS),[13] photodissociation processes are assumed to take place at fixed angles γ. If we consider the continuum wavefunctions without closed channel contributions, or without $n=1$ channel contributions, IOS continuum wavefunctions satisfy the following ordinary differential equations

$$\left[-\frac{1}{2m}\frac{\partial^2}{\partial R^2}+\frac{l^2}{2\mu R^2}+B_j^2+E_{v=0}+V_0(R,\ \gamma)\right]\Psi^{IOS}(R|\gamma)$$
$$=E\Psi^{IOS}(R/\gamma), \tag{71}$$

where $E_{v=0}$ is the vibrational energy of the diatomic molecule. As mentioned earlier, $J=0$ was assumed and j and l have identical values of, let us say, j_0. That is, $j^2=l^2=j_0(j_0+1)$ where j_0 is an arbitrary positive integer. The exact value of j_0 is not important. The reason for this may be easily understood if IOS wavefunctions are understood as wavefunctions at short-ranges where potential is highly negative and the rotational energy is much smaller than the kinetic energy of the relative motion along the dissociation coordinate R. IOS wavefunctions Ψ^{IOS} should satisfy the incoming wave boundary conditions

$$\Psi^{IOS}(R|\gamma)\rightarrow k_0^{-1/2}[e^{ik_0R}+S_0\ e^{-ik_0R}]$$
$$\rightarrow 2k^{-1/2}\ e^{-i\eta(\gamma)}\cos[k_0R+\eta(\gamma))],\ \text{as}\ R\rightarrow\infty \tag{72}$$

where η is the phase shift at the given angle γ. With this IOS wavefunction, $\Psi_c^{-(j)}(R,\ r,\ \gamma)$ may be obtained as

$$\Psi_c^{-(j)}(R,\ r,\ \gamma)=\Psi_c^{-(j)}(R,\ \gamma)\langle r|0\rangle=\Psi^{IOS}(R|\gamma)Y_{j0}(\gamma,\ 0)\langle r|0\rangle, \tag{73}$$

as can be confirmed by the examination of the boundary conditions they satisfy

$$Y_{j0}(\gamma,\ 0)\Psi^{IOS}(R|\gamma)\rightarrow k_j^{-1/2}[e^{ik_jR}Y_{j0}(\gamma,\ 0)+e^{-ik_jR}Y_{j0}(\gamma,\ 0)S_j^{IOS}(\gamma)]$$
$$\rightarrow k_j^{-1/2}[e^{ik_jR}Y_{j0}(\gamma,\ 0)+\sum_{j'}Y_{j'0}(\gamma,\ 0)S_{j'j}^{IOS}e^{-ik_jR}]$$
$$\rightarrow\sum_{j'}Y_{j'0}(\gamma,\ 0)\{k_{j'}^{-1/2}[e^{ik_{j'}R}\delta_{j'j}+S_{j'j}^{IOS}e^{-ik_jR}]\}$$
$$=\Psi^{-(j)}(R,\ \gamma). \tag{74}$$

Then

$$(\phi_b|V|\Psi_c^{-(j)})\approx(\phi_b|V|Y_{j0}\Psi^{IOS})|n=0\rangle$$
$$\approx\langle 1/r-r_e|0\rangle 2\pi\int_0^\pi d\gamma\sin\gamma Y_{j0}(\gamma,\ 0)A(\gamma)e^{i\eta(\gamma)} \tag{75}$$

where $A(\gamma)$ is given by

$$A(\gamma)\exp[i\eta(\gamma)]=\int_0^\infty dR\phi_b(R,\ \gamma)\left[\frac{\partial V}{\partial r}\right]_{r=r_e}\psi^{IOS}(R|\gamma)$$
$$=\int dR\sum_{j'}Y_{j'0}(\gamma,\ 0)\chi_{bj'}(R)\left[\frac{\partial V}{\partial r}\right]_{r=r_e}\Psi^{IOS}(R|\gamma). \tag{76}$$

Results and Discussion

Studies on the energy dependence of qdt parameters were thoroughly studied in the previous paper.[5] Only one of qdt parameters, the transition dipole moment, was not studied there. But before discussing the results of calculations of transition dipole moments, let us mention one missing point not dealt in the previous paper. In the previous work, it was noticed that some qdt parameters μ_α are crossing and others are avoiding each other as functions of energy. Since there is no symmetry in qdt parameters with respect to energy, any μ_α should avoid each other. The reason why some μ_α do not seem to be avoiding derives from the fact that μ_α's are periodic with period of 1 and that the range of energies examined was very narrow. In Figure 3, behaviors of μ_α are examined for a wide range of energies including threshold[14] regions for some channels. The figure shows that μ_α approaches zero as energy approaches the threshold. The

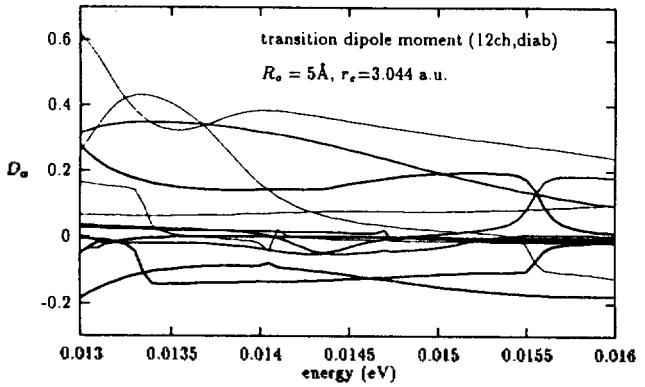

Figure 2. Transition dipole moments D_α *vs.* energy when 12 channels (6 open 6 closed) are included (R_e=5 Å, r_e=3.044 a.u.).

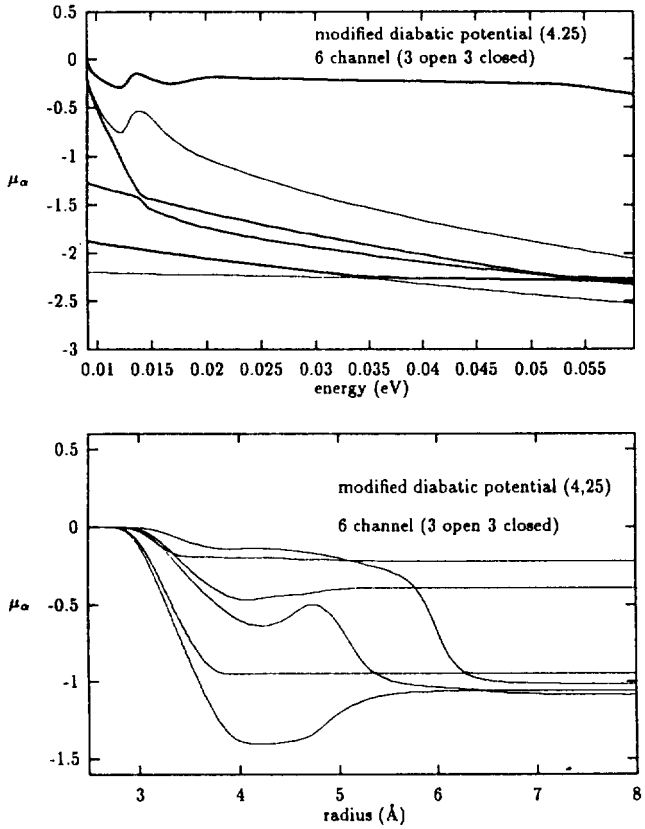

Figure 3. The first graph is for μ_α *vs.* energy for 6 channel cases (R_e=5 Å) while the second graph is for μ_α *vs.* R at E= 0.013 eV.

figure also shows that μ_α crossing each other in Figure 2 in Ref. 5 are no longer crossing owing to their translations by integers.

For the triatomic van der Waals molecules considered in this work, about twelve channels (6 open and 6 closed) are enough to obtain the convergence. Table 6 shows the first resonance energies and the rotational distributions of their wave functions given by P_{bj} in Eq. (65) as the number of channels are increased from 2 to 6 for r_e=3.044 a.u. and 5.044 a.u., respectively. MQDT and close coupling calculations showed the convergence at the similar number of chan-

Table 6. Resonance energies and proportions of rotational channels in the quasi bound states as functions of the closed channel numbers when diatomic bond lengths are 3.044 a.u and 5.044 a.u.

r_e=3.044 a.u.							
# of closed channels	the first resonance energy (eV)	proportions of rotational channels					
		0	2	4	6	8	10
2	0.0139677	1.00	0.31				
3	0.0134165	1.00	0.60	0.09			
4	0.0132496	1.00	0.70	0.19	0.02		
5	0.0132093	1.00	0.72	0.22	0.04	0.00	
6	0.0132026	1.00	0.73	0.22	0.04	0.00	0.00
r_e=5.044 a.u.							
# of closed channels	the first resonance energy (eV)	proportions of rotational channels					
		0	2	4	6	8	10
2	0.0139638	1.00	0.31				
3	0.0134165	1.00	0.60	0.09			
5	0.0135938	1.00	0.82	0.31	0.06	0.01	
6	0.0135341	1.00	0.84	0.34	0.09	0.01	
7	0.0135203	1.00	0.84	0.35	0.10	0.02	0.00
8	0.0135179	1.00	0.84	0.35	0.10	0.02	0.00

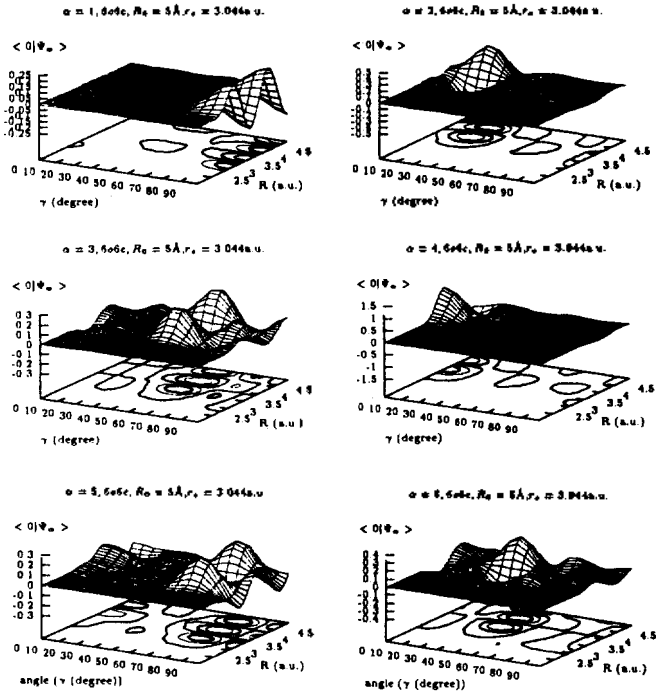

Figure 4. Short-range channel basis functions $\Psi_\alpha(E)$.

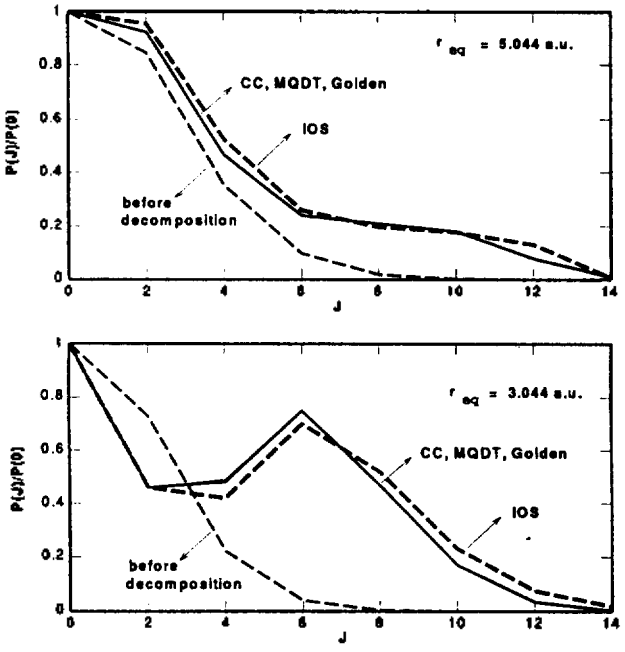

Figure 5. Comparison of final rotational distributions of photofragments normalized to the case of J=0 calculated by close coupling method, MQDT, Golden-rule like method, IOS approximation for r_e=5.044 a.u. and 3.044 a.u.. Calculation is done with 16 channels (8 open 8 closed). Also shown are the normalized probabilities of finding J in the quasi-bound state defined in Eq. (65).

nels.

The transition dipole moments D_α *vs.* energy for 12 channels are shown in Figure 1. Their variations as a function of energy are much bigger than those of other short range qdt parameters μ_α and $U_{i\alpha}$ but still small enough to be considered constant around resonances. As we described earlier, $U_{i\alpha}(i=1, 2,\cdots,n)$ represent the projections of the short range channel basis function Ψ_α to the standing wave channel basis functions Ψ_i or, if we disregard the unimportant phase factors, to the dissociation states $\Psi^{-(i)}$ to the channels i (i=1, 2,$\cdots$,n). Examination of $U_{i\alpha}$ shows that D_α is bigger as the

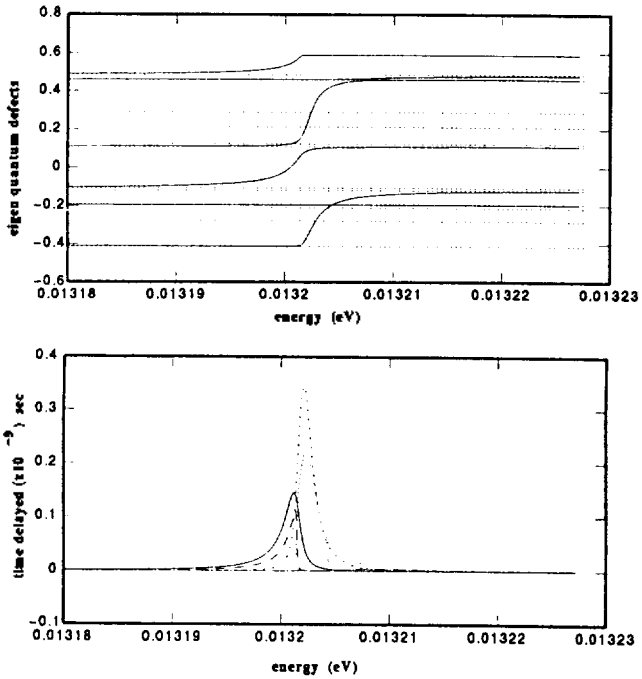

Figure 6. Eigenquantum defects μ_α and τ_ρ calculated around the resonance energy 0.0132026 eV with 12 channels (6 open 6 closed) and with r_e=3.044 a.u. are shown in the first graph. τ_ρ are shown by solid lines while μ_α are shown by dashed lines. The second graph shows times delayed by resonances for each eigen channel ρ.

closed channel contributions to α are bigger. As shown in Figure 4 for the first 6 α's (the remaining 6 Ψ_α are almost identical with the first 6 ones except the sign changes for n=1 components which are not shown), short range channel basis functions have values only around some angle values and may be regarded as angle functions. Then the values of D_α are big when Ψ_α correspond to angle functions which have big values around γ=90°. Since all the dynamics, such as energy exchanges, angular momentum transfers, torques exerting to the diatomic photofragments, occur when the photofragments are close together, we could approximate the states of the system during photodissociation by short-range eigenchannel basis functions Ψ_α. Since Ψ_α are angles functions, we may say that photodissociations occur along some angles whose values are fixed by Ψ_α. This picture is equivalent to the IOS approximation but differ in that now angles are quantized.

In MQDT, the effect of closed channels on the predissociation dynamics can be seen from the comparison of eigen quantum defects μ_α and τ_ρ. They are equal if the closed channels play no significant role either by their absence or at off-resonance. Figure 6 confirms this by showing that they differ only around a resonance. The first derivatives of τ_ρ with respect to E may show the net effects of closed channels. We notice that those quantities multiplied by $\hbar/2$, *i.e.* $(\hbar d\tau_\rho/2dE)$, are just the times delayed by collision at eigenchannels ρ.[15] The times delayed *vs.* E are shown in Figure 6. Notice that the magnitudes of times delayed agree quite well with 3.0×10^{-9} sec obtained from $\Gamma=2.2\times10^{-6}$ eV.

Table 7. The positions and widths of resonance peaks in case of 8, 10, 12 channels calculated by several methods (r_e=3.044 a.u.)

8 channels				
	Golden	IOS	Close-coupled	MQDT
E_r (eV)	0.0132494		0.0132490	0.0132486
Γ (eV)	1.46×10^{-6}	1.04×10^{-6}	1.0×10^{-6}	1.0×10^{-6}
10 channels				
	Golden	IOS	Close-coupled	MQDT
E_r (eV)	0.0132075		0.0132095	0.0132089
Γ (eV)	1.86×10^{-6}	1.72×10^{-6}	1.8×10^{-6}	2.0×10^{-6}
12 channels				
	Golden	IOS	Close-coupled	MQDT
E_r (eV)	0.0132026		0.0132024	0.0132021
Γ (eV)	2.19×10^{-6}	2.62×10^{-6}	2.2×10^{-6}	2.2×10^{-6}

Photodissociation cross sections calculated for the system of triatomic van der Waals molecules with the molecular parameters given in Table 1 and 2 take the Lorentzian shape around resonances. This is due to the fact that in the vibrational predissociation of van der Waals molecules the transition to the quasi-bound state is much bigger than that to the continuum states. The calculation of the line profile parameter q for the same system with molecular parameters given by Table 1 and 2 was −350, which indicates that the spectral shape is almost Lorentzian. Detailed study on this was published in the previous paper.[16] Table 7 summarizes the positions and widths of the resonance peaks in cases of 8, 10, 12 channels (consisting of half-open and half-closed channels) calculated by using the four different methods, Golden rule like calculation, IOS approximation, close coupling (CC) method, and MQDT method. The agreements among different methods are excellent. The table shows that the life times decrease or the resonance widths Γ increase with the increase of the number of channels. This looks reasonable since more channels mean more pathways to decompose.

The final rotational state distributions in case of r_e=3.044 a.u. and 5.044 a.u. calculated by four methods are shown in Figure 5. Also shown are the rotational state distributions of the diatomic molecule component in the triatomic van der Waals molecules at their quasi bound states. The binodal structures are shown up in case of r_e=3.044 a.u.. The figures show that the Golden-rule like calculation, the close coupling method, and the MQDT method yield almost identical results while the IOS approximation shows a little deviation. The IOS approximation shows the rotational distributions extended to higher J though such extensions are small. Uncertainty principle $\Delta J/\Delta\theta\sim\hbar$ tells us that a little extension to higher J means that angular motions in IOS are treated more rigidly than in other methods as can be understood intuitively.

The rotational state distributions of diatomic molecules at quasi bound states and at the photofragments are quite

different and those of the latter are more shifted to higher j values. That is, diatomic photofragments get more rotational angular momentum by the action of the torque of the anisotropy of the intermolecular potential as they depart from other fragment.

We can see from Table 7 that the resonance width in the molecular parameters chosen is around 2×10^{-6} eV and about ten times smaller than the value of rotational constant, 16.2×10^{-6} eV. That is, the resonance life time is more than ten times larger than the rotational period. It may be considered that resonance states live long enough to forget the ground state information. The fact that IOS approximation holds well means that the decomposition takes place much faster than the rotation of the diatomic fragment. This derives from the fact that the kinetic energy of the relative motion of photofragments is thousand times larger than the rotational energy.

Acknowledgment. This work was supported by KOSEF under Contract No. 913-0303-001-2.

References

1. Beneventi, L.; Casavecchia, P.; Volpi, G. G.; Bieler, C. R.; Janda, K. C. *J. Chem. Phys.* **1993**, *98*, 178 and references therein.
2. Schinke, R.; Engel, V. *Faraday Discuss. Chem. Soc.* **1986**, *82*, paper 11.
3. (a) Miller, W. H. *Adv. Chem. Phys.* **1975**, *25*, 69. (b) *ibid* **1975**, *30*, 77.
4. Fano, U.; Rau, A. R. P. *Atomic Collisions and Spectra*; Academic: Orlando, 1986.
5. Lee, C. W. *Bull. Korean Chem. Soc.* **1991**, *12*, 228.
6. Greene, C. H.; Rau, A. R. P.; Fano, U. *Phys. Rev.* **1982**, *A26*, 2441.
7. (a) See reference 2. (b) Buckingham, A. D.; Fowler, P. W.; Hutson, J. M. *Chem. Rev.* **1988**, *88*, 963.
8. Halberstadt, N.; Beswick, J. A.; Janda, K. C. *J. Chem. Phys.* **1987**, *87*, 3966.
9. Child, M. S. *Molecular Collision Theory*; Academic: London, 1974.
10. Lester, W. *Methods. Comput. Phys.* **1971**, *10*, 243.
11. Hager, W. W. *Applied Numerical Linear Algebra*; Prentice-Hall International: London, 1988.
12. Janda, K. C. *Adv. Chem. Phys.* **1985**, *20*, 201.
13. (a) McGuire, P. *Chem. Phys. Lett.* **1973**, *23*, 575. (b) Mcguire, P.; Kouri, D. J. *J. Chem. Phys.* **1974**, *60*, 2488. (c) Pack, R. T. *J. Chem. Phys.* **1974**, *60*, 633. (d) Schinke, R. *J. Phys. Chem.* **1986**, *90*, 1742.
14. Taylor, J. R. *Scattering Theory*; John Wiley and Sons: New York, 1972.
15. Smith, F. T. *J. Chem. Phys.* **1962**, *36*, 248.
16. Lee, C. W. *Bull. Korean. Chem. Soc.* **1995**, *20*, 850.

Assignment of the Redox Potentials of Cytochrome c_3 of *Desulfovibrio vulgaris* Hildenborough by ^{1}H NMR

Jang-Su Park*, Shin Won Kang, and Jung-Hyu Shin†

Department of chemistry, College of Natural Sciences, Pusan National University, Pusan 609-735, Korea
†Department of Chemistry, Seoul National University, Seoul 151-742, Korea
Received July 3, 1995

The heme assignment of the ^{1}H NMR spectrum of cytochrome c_3 of *Desulfovibrio vulgaris* Hildenborough within the X-ray structure were fully cross established according to their redox potential. The major reduction of the heme turned out to take place in the order of hemes IV, I, II and III (the heme numbers indicating the order of bonding to the primary sequence). This assignment can provide the physicochemical basis for the elucidation of electron transfer of this protein.

Introduction

Cytochrome c_3 are a family of low molecular weight (13 kDa) electron-transfer protein that may be isolated from sulfate-reducing bacteria.[1,2] The proteins contain 4 hemes in a single polypeptide and show very low redox potentials.[3] Cytochrome c_3 are electron carriers required for the electron transfer between hydrogenases[4] and smaller carriers. *In vitro*, they facilitate the electron transfer from hydrogenase to flavodoxin and rubredoxin[5] and are a necessary component of several different redox reaction in crude extracts.

*To whom correspondances should be addressed.

Crystal structures of cytochrome c_3 from *Desulfovibrio desulfuricans* Norway (*Dd*N), *Desulfovibrio vulgaris* Miyazaki F (*Dv*MF) and *Desulfovibrio vulgaris* Hildenborough (*Dv*H).[6~9] The two proteins are closely homologous. The redox potential of cytochrome c_3 is an important parameter in understanding its physiological role. Macroscopic and microscopic redox potentials were determined for a series of cytochrome c_3.[10~13] The assignment for *Dv*MF cytochrome c_3 of the microscopic redox potentials to the hemes in the crystal structure has been performed by means of NMR.[14] A correlation between the microscopic redox potentials and the crystal structure has been reported for cytochrome c_3 from *Dd*N.[15] It is interesting to compar the redox processes of two cy-